Iron oxidation and hydrolysis reactions of a novel ferritin from *Listeria innocua*

Xiaoke YANG*, Emilia CHIANCONE†, Simonetta STEFANINI†, Andrea ILARI† and N. Dennis CHASTEEN*[1]

*Department of Chemistry, Parsons Hall, University of New Hampshire, Durham, NH 03824, U.S.A., and †C.S. Biologia Molecolare, Dipartimento di Scienze Biochimiche 'A. Rossi Fanelli', Università di Roma 'La Sapienza', 00185 Rome, Italy

Iron deposition in the unusual 12-subunit ferritin from the bacterium *Listeria innocua* proceeds in three phases: a rapid first phase in which Fe^{2+} binds to the apoprotein, P^Z of charge Z, according to the postulated reaction $2Fe^{2+} + P^Z \rightarrow [Fe_2–P]^{Z+2} + 2H^+$, where $[Fe_2–P]^{Z+2}$ represents a dinuclear iron(II) complex formed at each of the 12 ferroxidase centres of the protein; a second phase corresponding to oxidation of this putative complex, i.e. $[Fe_2–P]^{Z+2} + \frac{1}{2}O_2 \rightarrow [Fe_2O–P]^Z + 2H^+$; and a third phase of iron(II) oxidation/mineralization, i.e. $4Fe^{2+} + O_2 + 8H_2O \rightarrow 8FeOOH_{(s)} + 8H^+$ [where $FeOOH_{(s)}$ represents the hydrous ferric oxide mineral that precipitates from the solution], which occurs when iron is added in excess of $24Fe^{2+}$/protein. In contrast with other ferritins, the ferroxidation reaction in *L. innocua* ferritin proceeds more slowly than the oxidation/mineralization reaction. Water is the final product of dioxygen reduction in the 12-subunit *L. innocua* ferritin (the present work) and in the 24-subunit *Escherichia coli* bacterioferritin, whereas H_2O_2 is produced in 24-subunit mammalian ferritins. Possible reasons for this difference are discussed.

Key words: iron mineralization, iron storage, oximetry, pH stat.

INTRODUCTION

The ferritins are a diverse group of iron(III) sequestering and storage proteins that are found widely distributed among animals, plants and microbes [1–3]. Most ferritins have an M_r close to 480000, and are composed of 24 similar or identical subunits that assemble to form a large shell-like structure of 4:3:2 octahedral symmetry. Iron is deposited within the protein cavity as a hydrous ferric oxide mineral containing various amounts of phosphate. Recently, an unusual ferritin has been discovered in the Gram-positive bacterium *Listeria innocua* [4,5]. *L. innocua* ferritin differs significantly from other known ferritins in that its protein shell is assembled from 12 identical subunits ($M_r \sim 18000$) to form a hollow structure having an M_r of ~ 240000 and 3:2 tetrahedral symmetry. This dodecameric (12mer) ferritin can rapidly accumulate 500 iron atoms within its central cavity, an amount far less than the maximum of 4500 Fe atoms found for the more common icosatetramer (24mer) ferritins, which have 8-fold larger cavity volumes [4,5]. *L. innocua* ferritin is similar in sequence and structure to the Dps proteins, a class of DNA-binding proteins that is expressed by bacteria under conditions of oxidative or nutritional stress [4].

Mammalian ferritins consist of two types of subunits, H and L, of similar sequence and M_r (~ 19000–21000). The H-subunit contains a dinuclear ferroxidase centre that promotes the pairwise oxidation of Fe^{2+} to Fe^{3+} and is located within the four-helix bundle of the subunit. The more acidic L-subunit lacks such a centre, but contains a number of glutamate residues on the inner surface of the protein shell that are believed to constitute a nucleation site for Fe^{3+} mineralization [3,6]. Dinuclear ferroxidase centres are also found in the four-helix bundle of the single type of subunit in the haem-containing 24mer bacterioferritins from *Escherichia coli* and *Azotobacter vinelandii* [2,7,8]. Recent X-ray structural studies of *L. innocua* ferritin have revealed that this ferritin likewise possesses iron-binding sites that are located at the interfaces of subunits related by two-fold symmetry [9,10]. The nature and stereochemistry of the iron-binding ligands resemble those of known ferroxidase sites. However, they are not found in a four-helix bundle, but are provided by two symmetry-related subunits. His-31, His-43 and Asp-47 are furnished by one subunit, and residues Asp-58 and Glu-62 by the other. The protein also has a cluster of acidic residues facing the inner surface of the protein cavity, reminiscent of the nucleation site of mammalian L-subunits [6].

The iron oxidation and hydrolysis chemistries of mammalian ferritin and bacterioferritin have been investigated extensively and are markedly different in several aspects [11–15]. Most importantly, hydrogen peroxide is the end product of dioxygen reduction in mammalian ferritins, whereas water is produced in bacterioferritin. Moreover, ferroxidase activity is regenerated in mammalian ferritin, but not in bacterioferritin [11,15]. Initial Fe^{2+} binding to the two types of ferritin also differs in the number of protons released [11,15].

The iron oxidation and hydrolysis reactions of the structurally unique *L. innocua* ferritin have not been investigated previously, and there are only limited data on the kinetics of iron deposition within the protein [5]. We report here the kinetics and stoichiometric equations for the ferroxidase and mineralization reactions of *L. innocua* ferritin. The data reveal that the overall mechanism of iron deposition in *L. innocua* ferritin more closely resembles that of bacterioferritin than that of mammalian ferritin, but differs in certain aspects from that of either.

EXPERIMENTAL

Listeria ferritin was isolated and purified and rendered iron-free as previously reported [4,5]. Apoferritin concentrations were determined spectrophotometrically using a molar absorptivity of 2.59×10^5 $M^{-1} \cdot cm^{-1}$ at 280 nm on a 12mer protein basis [5]. Freshly prepared solutions of hydrogen peroxide were assayed for H_2O_2 concentration using a Clarke oxygen electrode to measure the amount of O_2 liberated upon addition of bovine catalase (Boehringer-Mannheim) to the H_2O_2 solution. All chemicals were reagent grade or better, and were used without further purification.

[1] To whom correspondence should be addressed (e-mail ndc@cisunix.unh.edu).

The iron(II) oxidation and hydrolysis reactions were followed using a specially designed apparatus interfaced to a microcomputer and consisting of a pH-stat autotitrator, an oxygen meter and a hermetically sealed microcell containing Clarke-type oxygen, pH glass and Ag/AgCl reference microelectrodes within a stirred volume of 0.48 ml [11]. The apparatus enables one to measure simultaneously the kinetics of both O_2 consumption and H^+ production under buffer-free conditions when Fe^{2+} is introduced into the protein to initiate iron oxidation and mineralization. Overall reaction stoichiometries are computed from the total O_2 consumed and acid produced when the reaction is complete. The calculations assume complete oxidation of the iron. Since the oxygen and pH microelectrodes have response half-lives of 2.3 and 0.8 s respectively, the rates of reactions with half-lives shorter than about 5 s cannot be reliably measured with the apparatus. Typical conditions for the experiments were: 4 μM or 8 μM ferritin in 50 mM NaCl, pH stat = 7.0, with 24, 48 or 96 Fe^{2+} added per protein as freshly prepared 20 mM $FeSO_4$ (Baker Scientific). Further details of the apparatus and methodologies employed are described elsewhere [11].

RESULTS

Previous studies of *E. coli* bacterioferritin have shown that mineralization occurs in three phases. A rapid first phase corresponds to Fe^{2+} binding to the ferroxidase centre, and a slower second phase corresponds to iron oxidation at this centre [15]. The slowest third phase corresponds to core oxidation/mineralization, and only occurs when iron is added in excess of 48 Fe/apoprotein, the amount needed to saturate the 24 dinuclear ferroxidase centres on the protein. As demonstrated below, three phases are likewise observed during iron uptake in *L. innocua* ferritin. The phase 1 and 2 reactions of *L. innocua* ferritin are also postulated to occur at the ferroxidase centres of the protein, as found for bacterioferritin and mammalian ferritins [1–3, 11,12,15,16]. However, *L. innocua* ferritin is unique in that its phase 2 ferroxidation reaction proceeds more slowly than its phase 3 oxidation/mineralization reaction.

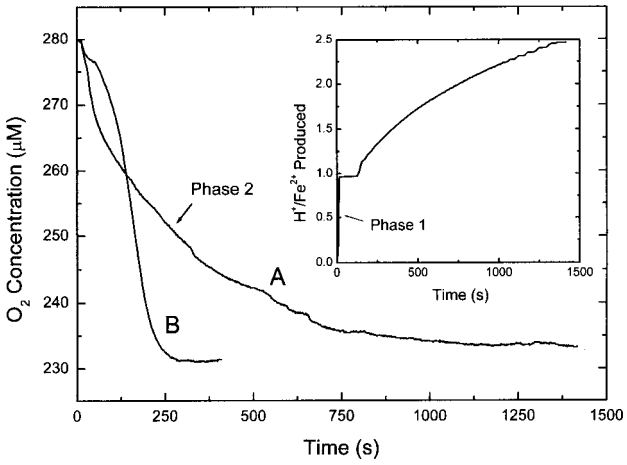

Figure 1 Oxygen consumption curves for ferroxidation in *L. innocua* ferritin at 24 Fe^{2+}/protein (curve A) and autoxidation in the absence of protein (curve B)

The inset shows proton production for the ferroxidation reaction (curve A). Conditions were 8 μM protein, 192 μM $FeSO_4$, 50 mM NaCl and pH stat 7.0, at 25 °C. Note that in the inset curve there is some initial overshoot of the pH-stat autotitrator by $\sim$ 10%, since the response of the apparatus cannot adequately track the fast reaction.

Phase 1 reaction

Figure 1 (curve A) shows the O_2 uptake curve for the ferroxidation reaction when 24 Fe^{2+} atoms are added to *L. innocua* apoferritin (8 μM apoprotein, 50 mM NaCl, pH stat 7.0), an amount required to completely occupy the 12 dinuclear ferroxidase sites of the protein. The inset of Figure 1 shows the corresponding H^+ production curve. There is an initial rapid production of H^+, corresponding to 0.94 H^+/Fe^{2+}, which occurs at a rate much higher than that of O_2 consumption (cf. curve A and inset in Figure 1). We ascribe this phenomenon to rapid Fe^{2+} binding to the protein and release of a proton, which must occur with a half-life of less than 0.8 s, the response time of the pH electrode. In bacterioferritin and human ferritin, Fe^{2+} binding to the protein occurs in less than 50 ms, as measured by stopped-flow kinetics [15,16]. Initial Fe^{2+} binding to *L. innocua* ferritin probably occurs at a similar high rate. Since nominally one proton is released per Fe^{2+} bound to the protein, we write the phase 1 reaction for *L. innocua* ferritin as:

$$2Fe^{2+} + P^z \rightarrow [Fe_2\text{–}P]^{z+2} + 2H^+ \quad (1)$$

where P^z and $[Fe_2\text{–}P]^{z+2}$ represent the vacant and Fe^{2+}-occupied ferroxidase centres on the protein respectively.

Phase 2 reaction

Curve B of Figure 1 is the O_2 uptake curve for the autoxidation reaction in the absence of protein when Fe^{2+} (196 μM) is added to the pH 7.0 saline solution. The curve for the autoxidation reaction (curve B) is sigmoidal, whereas that for the protein-assisted ferroxidation reaction (curve A) is largely hyperbolic. Similar observations were made previously when iron mineralization in *L. innocua* ferritin was followed spectrophotometrically at 310 nm [5]. The initial rate of Fe^{2+} oxidation in the presence of the protein is greater than that of autoxidation, but ultimately the rate of autoxidation, which is autocatalytic, exceeds the ferroxidation rate. The initial lag time seen in the sigmoidal curve for autoxidation corresponds to the time required to generate sufficient growing surface area of the polymeric iron upon which subsequent Fe^{2+} oxidation can occur [17]. A precipitate eventually forms during autoxidation, but not when the protein is present. Halving the protein and iron concentrations, while maintaining the Fe^{2+}/protein ratio at 24:1, causes the half-life of the phase 2 ferroxidation reaction to increase from $\sim$ 200 s (Figure 1, curve A) to $\sim$ 400 s (Figure 2, curve B). The half-lives for the ferroxidation reaction of human H-chain ferritin [11] and bacterioferritin [12] are much shorter than for *L. innocua* ferritin (10 s compared with 200 s) (Figure 1).

From the total amounts of O_2 consumed and H^+ produced at the end of the ferroxidase reaction (Figure 1, curve A), we obtain net stoichiometries of 4.1 ± 0.2 Fe^{2+}/O_2 and 2.3 ± 0.2 H^+/Fe^{2+}. Since nominally 1 H^+ is produced per Fe^{2+} binding to the protein (Figure 1, inset), the second H^+ per Fe^{2+} is produced during oxidation of the iron; its rate of production parallels the consumption of O_2 (Figure 1, cf. curve A and inset). We therefore write the phase 2 reaction as:

$$[Fe_2\text{–}P]^{z+2} + \tfrac{1}{2}O_2 \rightarrow [Fe_2O\text{–}P]^z + 2H^+ \quad (2)$$

where $[Fe_2O\text{–}P]^z$ represents an oxidized iron complex postulated to be at the ferroxidase centre. Since the data provide no information regarding the extent of hydration of the putative diFe^{3+} ferroxidase complex, the phase 2 reaction can alternatively be written as:

$$[Fe_2\text{–}P]^{z+2} + \tfrac{1}{2}O_2 + H_2O \rightarrow [Fe_2(OH)_2\text{–}P]^z + 2H^+ \quad (3)$$

For the autoxidation reaction (Figure 1, curve B), we obtained stoichiometries of 3.9 ± 0.1 Fe^{2+}/O_2 and 2.1 ± 0.1 H^+/Fe^{2+}. Thus

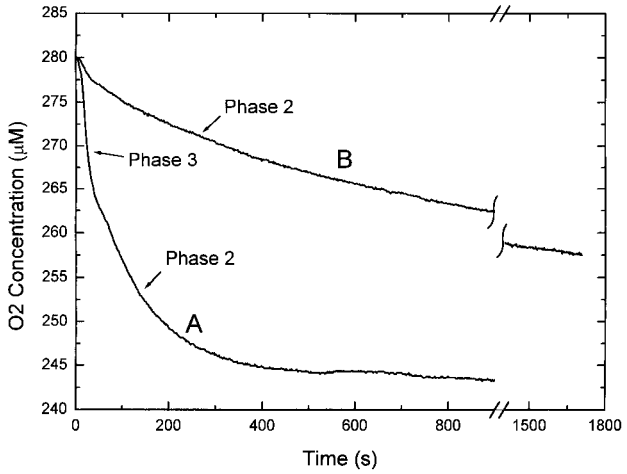

Figure 2 Oxygen consumption curves in the presence of 48 Fe^{2+}/apoprotein (curve A) and 24 Fe^{2+}/apoprotein (curve B)

Conditions were 4 μM protein, 50 mM NaCl and pH stat 7.0, at 25 °C.

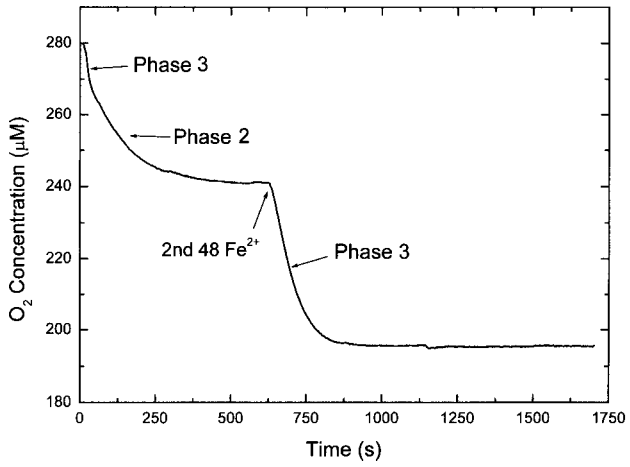

Figure 3 Oxygen consumption curve for two sequential additions of 48 Fe^{2+}/protein

Conditions were 4 μM protein, 50 mM NaCl and pH stat 7.0, at 25 °C.

the net reaction for autoxidation under the conditions of the experiment (192 μM $FeSO_4$, 50 mM NaCl, pH stat 7.0) is written as:

$$4Fe^{2+} + O_2 + 8H_2O \rightarrow 8FeOOH_{(s)} + 8H^+ \quad (4)$$

where $FeOOH_{(s)}$ represents the hydrous ferric oxide mineral that precipitates from the solution.

Phase 3 reaction

Curve A in Figure 2 illustrates the O_2 uptake curve when 48 Fe^{2+} are added to apoferritin (4 μM protein, 50 mM NaCl, pH stat 7.0). The O_2 uptake curve in this instance consists of two phases, each corresponding to approximately half of the Fe^{2+} oxidized. We attribute the faster phase to the phase 3 oxidation/mineralization reaction involving 24 Fe^{2+}, and the slower phase to the phase 2 ferroxidation reaction of the remaining 24 Fe^{2+}. This assignment is more evident from the data in Figure 3, where two additions of 48 Fe^{2+} are made to the same protein sample. Again, two phases are observed during the first addition of 48 Fe^{2+}, i.e. a faster oxidation/mineralization phase and a slower ferroxidation phase, but only the faster oxidation/mineralization phase is observed for the second addition of 48 Fe^{2+}.

When only 24 Fe^{2+} are added to the apoprotein under the same conditions as above, the phase 2 reaction proceeds slowly, with a half-life of $\sim$ 400 s and stoichiometries of 4.2 ± 0.3 Fe^{2+}/O_2 and 2.1 ± 0.2 H^+/Fe^{2+} (Figure 2, curve B). In the 48 Fe^{2+} sample, the presence of the additional 24 Fe^{2+} accelerates the phase 2 reaction, reducing its half-life from $\sim$ 400 to $\sim$ 90 s (Figure 2, curves A and B).

The apparent stoichiometries for the first 48 Fe^{2+}/protein addition in Figure 3 are 5.1 ± 0.2 Fe^{2+}/O_2 and 2.0 ± 0.2 H^+/Fe^{2+}. The high value of 5.1 for the Fe^{2+}/O_2 stoichiometry implies somewhat incomplete oxidation of the Fe^{2+} (less O_2 is consumed), a result consistent with a lower rate of oxidation at the ferroxidase centre. However, the stoichiometries for the second 48 Fe^{2+} addition are 3.6 ± 0.2 Fe^{2+}/O_2 (more O_2 is consumed) and 2.2 ± 0.2 H^+/Fe^{2+}, resulting in an average overall oxygen consumption stoichiometry for both additions of 4.3 ± 0.3 Fe^{2+}/O_2, close to the theoretical limiting value of 4.0. Accordingly, we write the phase 3 oxidation/mineralization reaction as:

$$4Fe^{2+} + O_2 + 8H_2O \rightarrow 8FeOOH_{(s)} + 8H^+ \quad (5)$$

which is the same as that for bacterioferritin and mammalian ferritins and for autoxidation [11–14,17,18].

Relative reactivities of O_2 and H_2O_2 towards Fe^{2+}

To test the relative reactivities of O_2 and H_2O_2 towards Fe^{2+} in *L. innocua* ferritin, 140 μM H_2O_2 was added to apoferritin (4 μM protein, 0.1 M NaCl, pH stat 7.0, 280 μM O_2). Then 48 Fe^{2+}/protein (192 μM) was added immediately, and the amount of O_2 consumed was measured and compared with the result obtained for the same experiment in the absence of H_2O_2. O_2 consumption was reduced by 75% in the presence of H_2O_2, a result implying that hydrogen peroxide is a significantly better oxidant for iron(II) in *L. innocua* ferritin than is dioxygen. A similar result was obtained with 192 μM Fe^{2+} in saline at pH 7.0 in the absence of protein, suggesting that H_2O_2 is also a superior oxidant for Fe^{2+} during autoxidation. Since Fe^{2+} oxidation by H_2O_2 is not measured directly in these experiments, it is not known whether the protein itself influences the oxidation rate. In contrast with the behaviour seen here, H_2O_2 does not appear to be a better oxidant than O_2 in mammalian ferritins, since the H_2O_2 produced at the ferroxidase centre in these proteins is released in solution and accumulates to measurable levels [11,13,18].

DISCUSSION

The iron oxidation and hydrolysis chemistry of *L. innocua* ferritin is similar in some aspects to the chemistry of other more thoroughly studied ferritins, but there are significant differences as well. In all ferritins, iron(II) added initially to the apoprotein is oxidized at the ferroxidase centres, except for recombinant L-chain homopolymers that lack such centres [6]. That the oxidation of the first 24 Fe^{2+} added to *L. innocua* ferritin occurs at the 12 ferroxidase centres of the protein is indicated by the marked difference in reaction kinetics when 24 compared with 48 Fe^{2+} are added (cf. curves A and B of Figure 2), the presence of two kinetic phases when 48 Fe^{2+} are added to the protein (Figure 2, curve A), each corresponding to approx. 24 Fe^{2+} being oxidized, and the fact that Tb^{3+}, a potent inhibitor of iron oxidation in *L. innocua* ferritin, also binds to the protein with a stoichiometric

ratio of $2Tb^{3+}$/subunit, the ratio expected for complexation at the dinuclear ferroxidase centre [5]. Tb^{3+} is also an inhibitor of iron oxidation in mammalian ferritins [13,14] and has been shown by X-ray crystallography to occupy the ferroxidase sites of recombinant human H-chain ferritin [19].

The rapid production of ~ 1 H^+/Fe^{2+} upon Fe^{2+} binding to *L. innocua* ferritin during the phase 1 reaction (Figure 1, inset) presumably arises from deprotonation of a protein ligand, since Fe^{2+} and its complexes normally are not hydrolysed at pH 7 [20]. In contrast, the proton counts for Fe^{2+} binding to horse spleen ferritin and *E. coli* bacterioferritin are 0.3 and 2.0 H^+/Fe^{2+} respectively [11,12]. These different values for the three proteins undoubtedly reflect differences in the detailed structures of their ferroxidase centres; most notably, the centres of the *E. coli* and *L. innocua* ferritins contain two histidine residues, whereas mammalian ferritins centres have only one [1–3,10]. There are other structural differences as well [1–3,10].

Similarly, in both *L. innocua* ferritin and *E. coli* bacterioferritin, dioxygen is completely reduced to water during both the ferroxidase (phase 2) and oxidation/mineralization (phase 3) reactions, whereas the ferroxidase reaction of mammalian ferritins produces hydrogen peroxide. Since hydrogen peroxide is the expected product of the two-electron oxidation of a diferrous complex at the ferroxidase centre, the failure to observe H_2O_2 production in *L. innocua* ferritin is perhaps due to H_2O_2 being a better oxidant for Fe^{2+} than is O_2 (see the Results section), as also found for *E. coli* bacterioferritin [12], but not for mammalian ferritin [11]. H_2O_2, if it were produced at one ferroxidase centre, may be rapidly consumed at another. Another possibility is that iron oxidation occurs via intermediate dinuclear Fe(IV) species in both *Listeria* ferritin and bacterioferritin [12]. The latter possibility is consistent with the failure to observe Fe turnover at the dinuclear centre, as suggested by the lack of regeneration of ferroxidase activity in both *Listeria* ferritin (Figure 3, second addition) and bacterioferritin [15]. Such inertness appears to be characteristic of high-valent dinuclear iron centres in enzymes such as methane mono-oxygenase that completely reduce dioxygen during their catalytic cycles (e.g. [21], see also [22]). In contrast, iron turnover occurs at the ferroxidase centres of animal ferritins, where hydrogen peroxide is produced [11,21,22].

The data for *L. innocua* ferritin also indicate that the overall process of Fe^{2+} oxidation at the ferroxidase centre is slower than both the autoxidation reaction taking place in the absence of protein (Figure 1) and the oxidation/mineralization reaction within the protein (Figures 2 and 3). However, binding of Fe^{2+} at the ferroxidase centres precedes the phase 3 oxidation/mineralization reaction, and possibly is a prerequisite for it to occur. Further studies with site-directed variants will establish whether this is the case and will also clarify the role of the protein in the chemistry observed here. Nevertheless, the present data suggest a synergism between the ferroxidation and the oxidation/mineralization reactions, since the rate of the former is increased when the latter is taking place (Figures 2 and 3). Conversely, when the ferroxidase centres are occupied by Tb(III), the rate of the overall process is decreased dramatically [5].

Another interesting observation is that the phase 3 oxidation/mineralization reaction of *L. innocua* ferritin at pH 7.0 (Figure 3) is about 2–4 times slower than that of *E. coli* bacterioferritin [12] at similar protein and iron concentrations. This phenomenon may reflect the smaller protein surface area available in the *Listeria* protein in comparison with the larger bacterial protein for promoting the mineral core reaction.

In conclusion, the present work has revealed several new features of the chemistry of iron deposition in *L. innocua* ferritin. In both the ferroxidation and oxidation/mineralization reactions, dioxygen is completely reduced to water, as also occurs in bacterioferritin, but not in mammalian ferritin. Thus, in contrast with mammalian ferritins, *Listeria* ferritin and *E. coli* bacterioferritin do not release H_2O_2 in solution, thereby preventing possible oxidative damage. In turn this feature is likely to be correlated with the absence of a nuclear membrane in prokaryotic cells, which renders the DNA more susceptible to oxidative damage. Even though the phase 2 ferroxidase reaction in *L. innocua* ferritin is unexpectedly slow, the protein nevertheless is capable of rapidly mineralizing iron through its phase 3 reaction. From the present work, it is evident that the various ferritins have evolved specialized structures that allow each of them to efficiently acquire iron from their environments, but they do so by somewhat different mechanisms. All ferritins, through formation of highly stable Fe^{3+} mineral cores within their central cavities, are able to fulfil one of their physiological functions, the protection of the organism against the toxic effects of 'free' iron.

This work was supported by grants R37 GM20194 from the National Institute of General Medical Sciences (N.D.C), and MURST grant 'Biologia strutturale e dinamica di proteine redox' (E.C.). Dr S. Cavallo is gratefully acknowledged for the preparation of the protein.

REFERENCES

1 Chasteen, N. D. and Harrison, P. M. (1999) J. Struct. Biol. **126**, 182–194
2 Andrews, S. C. (1999) Adv. Microb. Physiol. **40**, 281–351
3 Harrison, P. M. and Arosio, P. (1996) Biochim. Biophys. Acta Bioenergetics **1275**, 161–203
4 Bozzi, M., Mignogna, G., Stefanini, S., Barra, D., Longhi, C., Valenti, P. and Chiancone, E. (1997) J. Biol. Chem. **272**, 3259–3265
5 Stefanini, S., Cavallo, S., Montagnini, B. and Chianocone, E. (1999) Biochem. J. **338**, 71–75
6 Levi, S., Yewdall, S. J., Harrison, P. M., Santambrogio, P., Cozzi, A., Rovida, E., Albertini, A. and Arosio, P. (1992) Biochem. J. **288**, 591–596
7 Andrews, S. C., Smith, J. M. A., Yewdall, S. J., Guest, J. R. and Harrison, P. M. (1991) FEBS Lett. **293**, 164–168
8 Dautant, A., Meyer, J., Yariv, J., Precigoux, G., Sweet, R. M., Kalb, A. J. and Frolow, F. (1998) Acta Crystallogr. D **54**, 16–24
9 Ilari, A., Savino, C., Stefanini, S., Chiancone, E. and Tsernoglou, D. (1999) Acta Crystallogr. D **55**, 552–553
10 Ilari, A., Stefanini, S., Chiancone, E. and Tsernoglou, D. (2000) Nat. Struct. Biol. **7**, 38–43
11 Yang, X., Chen-Barrett, Y., Arosio, P. and Chasteen, N. D. (1998) Biochemistry **37**, 9743–9750
12 Yang, X., Le Brun, N. E., Thomson, A. J., Moore, G. and Chasteen, N. D. (2000) Biochemistry **39**, 4915–4923
13 Sun, S. and Chasteen, N. D. (1992) J. Biol. Chem **267**, 25160–25166
14 Sun, S., Arosio, P., Levi, S. and Chasteen, N. D. (1993) Biochemistry **32**, 9362–9369
15 Le Brun, N. E., Wilson, M. T., Andrews, S. C., Guest, J. R., Harrison, P. M., Thomson, A. J. and Moore, G. R. (1993) FEBS Lett. **333**, 197–202
16 Treffry, A., Zhao, A., Quail, M. A., Guest, J. R. and Harrison, P. M. (1997) Biochemistry **36**, 432–441
17 Yang, X. and Chasteen, N. D. (1999) Biochem. J. **338**, 615–618
18 Xu, B. and Chasteen, N. D. (1991) J. Biol. Chem. **266**, 19965–19970
19 Lawson, D. M., Artymiuk, P. J., Yewdall, S. J., Smith, J. M. A., Livingstone, J. C., Treffry, A., Luzzago, A., Levi, S., Arosio, P., Cesareni, G. et al. (1991) Nature (London) **349**, 541–544
20 Smith, R. M. and Martell, A. E. (1976) Critical Stability Constants, vol. 4, pp. 1 and 5, Plenum Press, New York
21 Hwang, J., Krebs, C., Huynh, B. H., Edmondson, D. E., Theil, E. C. and Penner-Hahn, J. E. (2000) Science **287**, 122–125
22 Hwang, J., Krebs, C., Huynh, B. H., Edmondson, D. E., Theil, E. C. and Penner-Hahn, J. E. (2000) Science **287**, 807 (erratum)

Received 13 March 2000; accepted 26 May 2000